Terrestrial gamma-ray flash electron beam geometry, fluence, and detection frequency

B. E. Carlson,[1] T. Gjesteland,[1] and N. Østgaard[1]

Received 6 May 2011; revised 9 September 2011; accepted 11 September 2011; published 19 November 2011.

[1] Terrestrial gamma-ray flashes (TGFs) are associated with emission of detectable beams of electrons into space. In this paper we use simulations of TGF and electron beam emission and escape from the atmosphere to determine how the geometry and fluence of such events depend on the angular distribution of the source photons. Given a photon source, the geometry of the electron beam depends on the geomagnetic latitude of the source but can be well-predicted by tracing a disk at 57 km altitude along the geomagnetic field to satellite orbit. The fluence and geometry are then used to infer the relative detection probabilities of TGF and electron beam in the context of a variety of photon sources and intensities. Analysis of detection probabilities and the relative frequency of TGF and electron beam detections suggests the existence of a population of electron beams emitted by TGFs too faint to be detected as photons.

Citation: Carlson, B. E., T. Gjesteland, and N. Østgaard (2011), Terrestrial gamma-ray flash electron beam geometry, fluence, and detection frequency, *J. Geophys. Res.*, *116*, A11217, doi:10.1029/2011JA016812.

1. Introduction

[2] Terrestrial gamma-ray flashes (TGFs) are brief pulses of photons observed by satellites [*Fishman et al.*, 1994; *Smith et al.*, 2005; *Marisaldi et al.*, 2010; *Briggs et al.*, 2010]. TGF photons have a very hard spectrum that can only be understood as bremsstrahlung from a source placed deep in Earth's atmosphere (altitude $\lesssim$ 20 km [see *Dwyer and Smith*, 2005; *Carlson et al.*, 2007; *Østgaard et al.*, 2008; *Gjesteland et al.*, 2010]). This source is likely closely associated with lightning as TGFs are typically coincident with observable thunderstorm electrical activity [*Inan et al.*, 1996; *Cohen et al.*, 2006; *Inan et al.*, 2006]. Geolocation of this electrical activity shows that lightning typically occurs within ~1 ms of the TGF and within a few hundred kilometers of the subsatellite point [*Cummer et al.*, 2005; *Stanley et al.*, 2006; *Cohen et al.*, 2010; *Connaughton et al.*, 2010]. Despite much study, the connection between TGFs and lightning is not fully understood. Most recent efforts focus on energetic electron behavior in the dynamic electric fields near an active lightning channel [*Moss et al.*, 2006; *Dwyer*, 2008; *Carlson et al.*, 2009a, 2010; *Chanrion and Neubert*, 2010; *Celestin and Pasko*, 2011] and on the weaker fields that carry higher overall electric potential that exist throughout a thundercloud [*Dwyer*, 2007, 2008], though a combination of such processes has also been suggested [*Moss et al.*, 2006; *Dwyer*, 2008].

[3] In spite of this theoretical and observational effort, the global frequency of TGF production is unknown. The observed frequency of satellite TGF observations sets a hard lower limit on the global frequency of 50/day assuming TGFs can be detected whenever they occur within 1000 km of the subsatellite point [*Smith et al.*, 2005]. Assuming TGFs are only detectable within 300 km as suggested by lightning geolocations cited above requires a global frequency above 500/day [*Carlson et al.*, 2009a]. Note that comparing 500 TGFs per day with the typical global lightning frequency of 45/s [*Christian*, 2003] indicates that on average at least 1 of every 10^4 lightning discharges produces a TGF. Such estimates of the true global frequency depend strongly on the width of the initial directional distribution (beaming) of the TGF photons. Narrow beams are less likely to be detected by satellites and require a higher global frequency to account for existing observations. The beaming of TGF photons also carries information about the geometry of the TGF source, with broader beams associated with divergent small-scale fields and narrower beams with relatively uniform large-scale fields. Unfortunately, the beam properties are not resolved in existing satellite measurements, though existing efforts point to broader beams [*Carlson et al.*, 2007; *Carlson*, 2009; *Hazelton et al.*, 2009; *Gjesteland et al.*, 2011]. As such, new sources of information are needed to address this topic.

[4] One such source of information is the electrons that escape to space along with the photons during a TGF. These electrons either directly come from the strong electric field regions that produce the TGF or are produced indirectly as a consequence of the physics of gamma-ray propagation in the atmosphere. TGF gamma-rays undergo Compton scattering, pair production, and photoelectric absorption to release energetic electrons. Regardless of the source, such electrons are only likely to escape the atmosphere if they are produced at high altitudes, at least above ~35 km where the collision frequency is less than the electron gyrofrequency [*Lehtinen et al.*, 1999]. As TGF photon emissions seem to originate at substantially lower altitudes, the electrons that escape to

[1]Department of Physics and Technology, University of Bergen, Bergen, Norway.

0148-0227/11/2011JA016812

satellite altitude are most likely secondary electrons produced by TGF photons [*Dwyer et al.*, 2008].

[5] Given that TGF photons both produce and are attenuated less than escaping electrons, relatively few electrons escape to satellite altitude. In spite of the smaller relative population size, the electron fluence remains comparable to the photon fluence because the geomagnetic field confines the escaping electrons to a much smaller region. While photons spread widely as they propagate to satellite altitude, electrons merely gyrate and travel along the geomagnetic field in a narrow beam. The result is a broad region of satellite orbit illuminated by gamma rays and a small region illuminated by electrons. A satellite within the region illuminated by gamma-rays will see a TGF, while a satellite struck by the electron beam will see a pulse of electrons and positrons with a broad energy distribution lasting ~5–25 ms depending on the distance along the geomagnetic field from source to satellite [*Dwyer et al.*, 2008; *Carlson et al.*, 2009b].

[6] Such events have been observed, though much less frequently than TGFs due to the small size of the electron beam. For example, observations made by the Burst and Transient Source Experiment (BATSE) on board the Compton Gamma-Ray Observatory of a TGF-like pulse of energetic particles over the Sahara Desert can be well-explained by modeling a beam of electrons produced by a TGF in the conjugate hemisphere, as can an event off the coast of Japan [*Dwyer et al.*, 2008]. The Gamma-ray Burst Monitor (GBM) on board the Fermi Gamma-ray Space Telescope has also seen such events and additionally measures a particle spectrum that shows a clear signature of positron annihilation in the spacecraft as would be produced if ~15% of the incoming particles were positrons [*Briggs et al.*, 2011]. Anomalous pulses of electrons observed by the SAMPEX spacecraft may also be TGF-associated electron beams [*Carlson et al.*, 2009b].

[7] In the context of TGF beaming and global frequency, the focus of this paper is the geometry, fluence, and frequency of observation of electron beams as a possible source of constraints on TGF properties. We approach this topic by assuming various initial photon populations and simulating the resulting photon and electron escape to satellite altitude, estimating the properties of satellite observations of these electrons, and calculating average observation probabilities over the observed TGF distributions. The resulting fluence and detection frequency estimates help us interpret the frequency of TGF and electron beam observations, allow us to crudely constrain the properties of the photon source, and will raise questions about satellite detection efficiency and the global frequency of TGFs.

2. Electron Beam Simulations

[8] The electron emissions described above are simulated with a combination of the GEANT4 Monte Carlo [*Agostinelli et al.*, 2003] and a deterministic guiding center motion simulation. Processes below 150 km altitude are handled with GEANT4, while electron and positron propagation above 150 km are handled with the guiding center motion simulation. The threshold of 150 km is chosen to limit the guiding center motion simulation to regions where electron motion is not significantly affected by collisions. The IGRF11 vector magnetic field model is used throughout [*Finlay et al.*, 2010], while the GEANT4 simulations include all relevant physics of photon and electron propagation in a MSIS atmosphere [*Hedin*, 1991] assumed constant around a spherical Earth. The simulations are started with a point source of photons directed upward with solid angle distribution $dN/d\Omega \propto \exp(-\theta^2/2\sigma_\theta^2)$ where θ is the zenith angle and σ_θ is a measure of the width of the beam. Such point sources provide a lower limit on the size of the emission region, while extended sources can be treated by expanding the size estimates given by point sources. The initial photon energy distribution is taken from relativistic runaway electron avalanche simulations consistent with TGF observations [*Carlson et al.*, 2007]. For simplicity, this spectrum is assumed not to vary significantly with direction as justified by very good spectral fits with nearly direction-independent spectra as in *Hazelton et al.*'s [2009] Figure 2. σ_θ ranges from 5° to 60°, ranging from unrealistically narrow (narrower than allowed by electron scattering and bremsstrahlung beaming) to unrealistically broad (such broad emissions cannot explain the observed average spectra) and including the range that best fits observed TGF spectra [*Carlson et al.*, 2007; *Hazelton et al.*, 2009; *Gjesteland et al.*, 2011]. The source is always placed at 20 km altitude, the highest altitude consistent with TGF spectra [*Dwyer and Smith*, 2005; *Carlson et al.*, 2007; *Gjesteland et al.*, 2010], though simulations at lower altitudes do not significantly alter our results. Photons that reach 550 km altitude are taken to have reached satellite orbit and are recorded. Electrons are recorded when they cross satellite altitude in both upward and downward directions, and are propagated until they either are absorbed by the atmosphere or are terminated by the simulation when they exceed a propagation time limit of 0.2 s. The net result of these simulations is a single record of photons reaching satellite altitude and a complete record of initial and subsequent electron crossings of satellite orbit up to the time limit.

[9] As we are interested in the frequency of detection of TGFs and electron beams, two results of the simulations are particularly relevant: the fluence (particles per area) of the emissions at satellite orbit and the area of satellite orbit illuminated by electrons and photons. The fluence of the emissions can easily be assessed by histogram or kernel density estimation. Example photon and electron fluence distributions at satellite altitude are shown in Figure 1. Electron fluence estimates are made in a plane perpendicular to the geomagnetic field and are propagated along the field to determine the corresponding fluence at satellite orbit. Photon fluence estimates are simply collected at satellite orbit. Note that the absolute fluence scale is arbitrary as the number of simulation particles is not the same as the number of particles in a TGF. However, the same fluence scale is used throughout Figure 1 and a single simulation gives both photons and electrons, so the relative fluence measurements in Figure 1 give the proper ratio of peak electron fluence to peak photon fluence. Provided the electron beam reaches satellite altitude, this ratio depends only weakly on the latitude and varies from 1 to 3, consistent with *Dwyer et al.* [2008], and varies slowly with the initial beam width (σ_θ).

[10] Figure 1 shows electron fluence distributions for several different TGF source latitudes. The variety of areas at satellite orbit illuminated by electrons indicates that electron

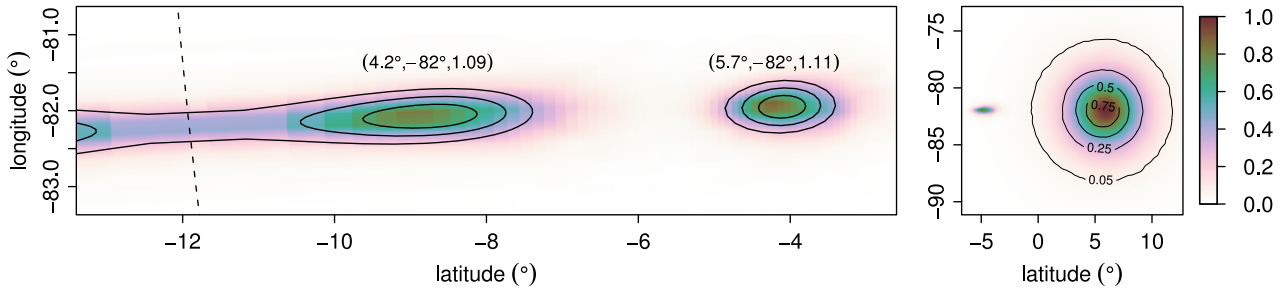

Figure 1. Sample electron and photon fluence at satellite orbit for simulations with $\sigma_\theta = 40°$. (left) Electron beam fluence. Each region of high fluence is labeled as (latitude, longitude, L-shell) with the location of the photon source that produced the electrons and the approximate L-shell of the electron beam. The contours result from tracing horizontal rings of radius 15 km, 25 km, and 35 km at 57 km altitude upward along the geomagnetic field to satellite altitude. The pattern roughly mirrors itself across the geomagnetic equator (shown as a dashed line). (right) Photon and electron fluence at satellite orbit for a photon source at (latitude, longitude) = (5.7°, −82°). The broad emission region is the TGF, while the narrow peak at left is the electron beam. The contours on the photon emission region refer to the photon fluence relative to the peak fluence.

beams emitted at different latitudes are not all equally likely to be detected. As such, estimates of electron beam detection probability depend strongly on the location of the source. The relevant area at satellite orbit can be determined directly by Monte Carlo particle simulations, but can also be estimated by tracing along the geomagnetic field from a ring placed at 57 km altitude above the source as shown by the lines in Figure 1. This is a straightforward method of estimating the position and size of the region at satellite orbit in which an electron beam is observable.

[11] The simulations in Figure 1 all used photons beamed upward with $\sigma_\theta = 40°$. Narrower or broader initial beams of photons will produce different size electron beams and will illuminate different size areas at satellite orbit. The effective size of a particular electron beam is determined by the instrument detection threshold and therefore depends on the absolute luminosity of the source and on the minimum fluence (particles per area) detectable by the instrument in a given time window. The quantity of interest then is the area illuminated by electrons and photons with a fluence higher than the minimum detectable fluence as a function of both σ_θ and the peak fluence. As such, we measure peak fluence in units of the minimum detectable fluence and determine the illuminated area as follows. For a given σ_θ we simulate a TGF and the associated electron beam. The fluence of photons and electrons at satellite altitude is calculated as in Figure 1. Contours of the fluence relative to the peak fluence are then calculated for electrons and photons and the area enclosed by the contours is measured. We then measure the effective radius of the photon beam at satellite orbit by simply calculating the radius of the circle with equivalent area. We measure the electron beam size as the radius of the circle that, when traced from some altitude above the source to satellite orbit, intersects an area that matches the area enclosed by the given relative fluence contour. These circle traces match the electron beam locations found in simulation if the circles are started at 57 km altitude centered above the source as shown in Figure 1. This area measurement procedure is executed for each σ_θ and each relative fluence contour to give a measure of the size of the electron and photon beams as a function of relative fluence and beaming angle, as desired. The relative fluence levels are then inverted to give the peak fluences (measured relative to the minimum detectable fluence) such that the given fluence contour falls at the minimum detectable fluence. These effective sizes are shown for four different σ_θ in Figure 2. Note that for low peak electron beam intensities (e.g. less than 2 × the minimum detectable fluence for σ_θ = 30°), the peak photon fluence is below the detection threshold

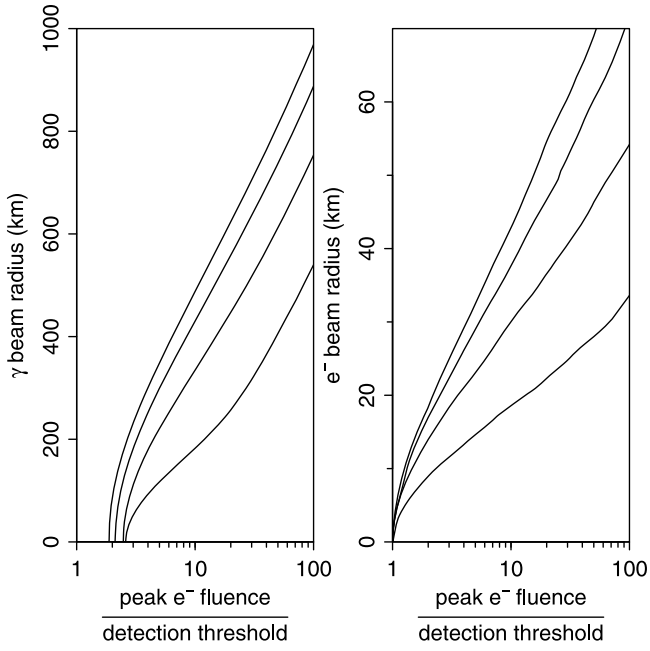

Figure 2. Effective photon and electron beam sizes at satellite orbit shown vs the peak electron beam fluence relative to the detection threshold assuming the minimum detectable photon and electron fluences are the same. The four curves shown in each plot correspond (top to bottom) to σ_θ = 40°, 30°, 20°, and 10°.